Inside Front Cover: Manipulating the Local Light Emission in Organic Light-Emitting Diodes by using Patterned Self-Assembled Monolayers (Adv. Mater. 14/2008)

ARTICLE *in* ADVANCED MATERIALS · JULY 2008

Impact Factor: 17.49 · DOI: 10.1002/adma.200890055 · Source: OAI

8 AUTHORS, INCLUDING:

Edsger Smits
Holst Centre
78 PUBLICATIONS **2,164** CITATIONS
SEE PROFILE

Martijn Kemerink
Linköping University
149 PUBLICATIONS **3,978** CITATIONS
SEE PROFILE

DOI: 10.1002/adma.200800299

Manipulating the Local Light Emission in Organic Light-Emitting Diodes by using Patterned Self-Assembled Monolayers**

By *Simon G. J. Mathijssen,* Paul A. van Hal, Ton J. M. van den Biggelaar, Edsger C. P. Smits, Bert de Boer, Martijn Kemerink, René A. J. Janssen,* and *Dago M. de Leeuw*

In organic light-emitting diodes (OLEDs), interface dipoles play an important role in the process of charge injection from the metallic electrode into the active organic layer.[1,2] An oriented dipole layer changes the effective work function of the electrode because of its internal electric field. The differences between the work functions of the electrodes and the highest occupied molecular orbital (HOMO) and lowest unoccupied molecular orbital (LUMO) of the light-emitting polymer determine the injection barriers and, thus, the electron/hole current balance and light emission of an OLED.[3] Therefore, the local light emission can be enhanced or suppressed by changing the work function on a local scale. This control of local emission is ideally suited for OLED-based signage applications, for example.

Here we use patterned, microcontact-printed (μCP) self-assembled monolayers (SAMs) with opposite dipole moments to change the local work function. This local work function change is analyzed by using scanning Kelvin probe microscopy (SKPM) with a lateral resolution on the order of 100 nm. We fabricate OLEDs with SAM-modified anodes and measure the light emission. By combining the SKPM measurements with optical microscopy images of the patterned OLEDs, we demonstrate a direct correlation between the local work function and light emission.

Patterned self-assembled monolayers were obtained using a poly(dimethylsiloxane) (PDMS, Sylgard 184, Dow Corning) stamp. The PDMS was poured onto a prepatterned mold and baked at 65 °C.[4] The stamps were put in an ethanol solution of either 2 mM 1-octadecanethiol ($C_{18}H_{37}SH$) or 2 mM 13,13,14,14,15,15,16,16,16-nonafluoro-1-hexadecanethiol ($C_4F_9C_{12}H_{24}SH$) for 1 h. Subsequently, the stamps were rinsed with ethanol and blown dry with nitrogen. The stamp, soaked with solution, was then pressed onto a gold electrode for 20 s, resulting in a patterned monolayer of either $C_{18}H_{37}SH$ (CH_3-SAM) or $C_4F_9C_{12}H_{24}SH$ (F-SAM), which are expected to have opposite dipole moments.

A single dipole layer on a metal, as provided by the stamped SAMs, can be modeled by two parallel sheets of charge Q separated by a distance d. The change in metal work function due to this dipole layer follows from classical electrostatics:

$$\Delta\phi = \frac{Qd}{A\varepsilon_0\varepsilon_{SAM}} = \frac{\sigma d}{\varepsilon_0\varepsilon_{SAM}} = N\frac{qd}{\varepsilon_0\varepsilon_{SAM}} = -N\frac{\mu_\perp}{\varepsilon_0\varepsilon_{SAM}} \quad (1)$$

in which ε corresponds to the permittivity of the dipole layer, ε_0 to the vacuum permittivity, σ to the charge per unit of area A, N to the number of molecules per unit area, and $\mu_\perp$ to the component of the dipole moment normal to the surface.[5] N is commonly known as the grafting density. A chemisorbed SAM on a metal is usually described by a superposition of two dipoles: one originating from the metal–sulfur (M–S) charge transfer interaction μ_{M-S} and one intrinsic to the molecule $\mu_{\perp,SAM}$.[6,7] According to recent density functional theory (DFT) calculations, the contribution of μ_{M-S} to the total dipole moment is much smaller than that of $\mu_{\perp,SAM}$, and therefore μ_{M-S} can be disregarded.[8–10] The magnitude of the dipole moment is mainly determined by the adsorbed molecule itself. Under this assumption, the change in surface potential, and therefore the change in work function of the electrode ($\chi_{electrode}$), can then be determined using[11,12]

$$\Delta V = -\Delta\chi_{electrode} = N\frac{\mu_{\perp,SAM}}{\varepsilon_0\varepsilon_{SAM}}. \quad (2)$$

The topography and work function of the patterned monolayers were measured using scanning Kelvin probe micro-

[*] S. G. J. Mathijssen, Dr. M. Kemerink, Prof. R. A. J. Janssen
Eindhoven University of Technology
Department of Applied Physics
P.O. Box 513
5600 MB Eindhoven (The Netherlands)
E-mail: s.g.j.mathijssen@tue.nl
S. G. J. Mathijssen, Dr. P. A. van Hal, A. J. M. van den Biggelaar, E. C. P. Smits, Prof. D. M. de Leeuw
Philips Research Laboratories
High Tech Campus 4
5656 AE Eindhoven (The Netherlands)
E. C. P. Smits, Dr. B. de Boer, Prof. D. M. de Leeuw
University of Groningen
Zernike Institute of Advanced Materials
Nijenborgh 4
9747 AG Groningen (The Netherlands)

[**] We thank H. Lifka and S. L. M. van Mensfoort for stimulating discussions. The authors gratefully acknowledge financial support from the EC (NAIMO NMP4-CT-2004-500355). The work of E.C.P.S. forms part of the Dutch Polymer Institute (DPI) research program (project no. 516). This research is supported by the Dutch Technology Foundation STW, applied science division of NWO and the Technology Program of the Ministry of Economic Affairs.

ADVANCED MATERIALS

scopy.[13–15] First a height profile was recorded by tapping-mode atomic force microscopy (AFM), followed by a second pass in which the work function was measured at a lift height of 25 nm above the surface. The work function was obtained by nullifying the frequency (ω) component of the electrostatic force (F_ω) on the tip: $F_\omega = \partial C/\partial z[(\Delta\chi - V_{dc})V_{ac}\sin(\omega t)]$, in which C is the capacitance between tip and sample, z the distance of the tip to the sample surface, and V_{ac} is the amplitude of the applied ac voltage signal. When the potential applied to the tip (V_{dc}) is equal to the work function difference between the tip and the sample surface, $\Delta\chi = \chi_{tip} - \chi_{sample}$, the electrostatic force is zero. Therefore, the work function between the tip and sample can be deduced directly from the applied potential on the tip, using $V_{dc} = \Delta\chi$.[13] In this manner, the local work function of both the printed monolayer and the surrounding gold were measured, with the untreated gold acting as an internal reference.

The height profiles of the microcontact-printed self-assembled monolayers of $C_{18}H_{37}SH$ and $C_4F_9C_{12}H_{24}SH$ are presented in Figure 1a and b, respectively. From the topography, a mean height difference of approximately 2 nm between the covered and uncovered regions for both molecules is deduced. These heights are, within experimental accuracy, in agreement with the length of the molecules. The off-normal tilt angle could not be accurately determined. The simultaneously measured potential profiles are presented in Figure 1c and d. We observe a direct correlation between the height and potential profile owing to the local change in surface potential caused by the dipole moments of the printed molecules. In Figure 1e curves A and B are cross-sections of the potential profiles for the $C_4F_9C_{12}H_{24}SH$ and $C_{18}H_{37}SH$ monolayers, respectively. We obtain a change of the surface potential of −0.3 V and 0.5 V for the F-SAM and CH_3-SAM covered regions. We calculate the work function change using $\chi_{SAM} - \chi_{Au} = V_{Au} - V_{SAM}$, in which χ is the work function and V the measured surface potential of either the Au or the SAM region (indicated by the subscript).[12] This implies that the effective work function of Au is changed from 4.9 eV to 5.2 eV and 4.4 eV in the case of the F-SAM and CH_3-SAM.

As argued above, we can calculate the expected work function change by using only the contribution of $\mu_{\perp,SAM}$. The C_{18}-alkanethiol has a calculated dipole moment along the surface normal of 1.5 D. The fluorinated alkanethiol, on the other hand, has a calculated dipole moment along the surface normal of −1.4 D.[16] Taking reported grafting densities of 4.6×10^{18} m^{-2} and 3.4×10^{18} m^{-2} and dielectric constants of 2.5 and 2.1 for the CH_3-SAM and F-SAM on gold, respectively,[10] we calculate from Equation 2 an expected surface potential change of 1.0 V and −0.85 V for the CH_3-SAM and F-SAM on gold. The measured changes in surface potential of the printed

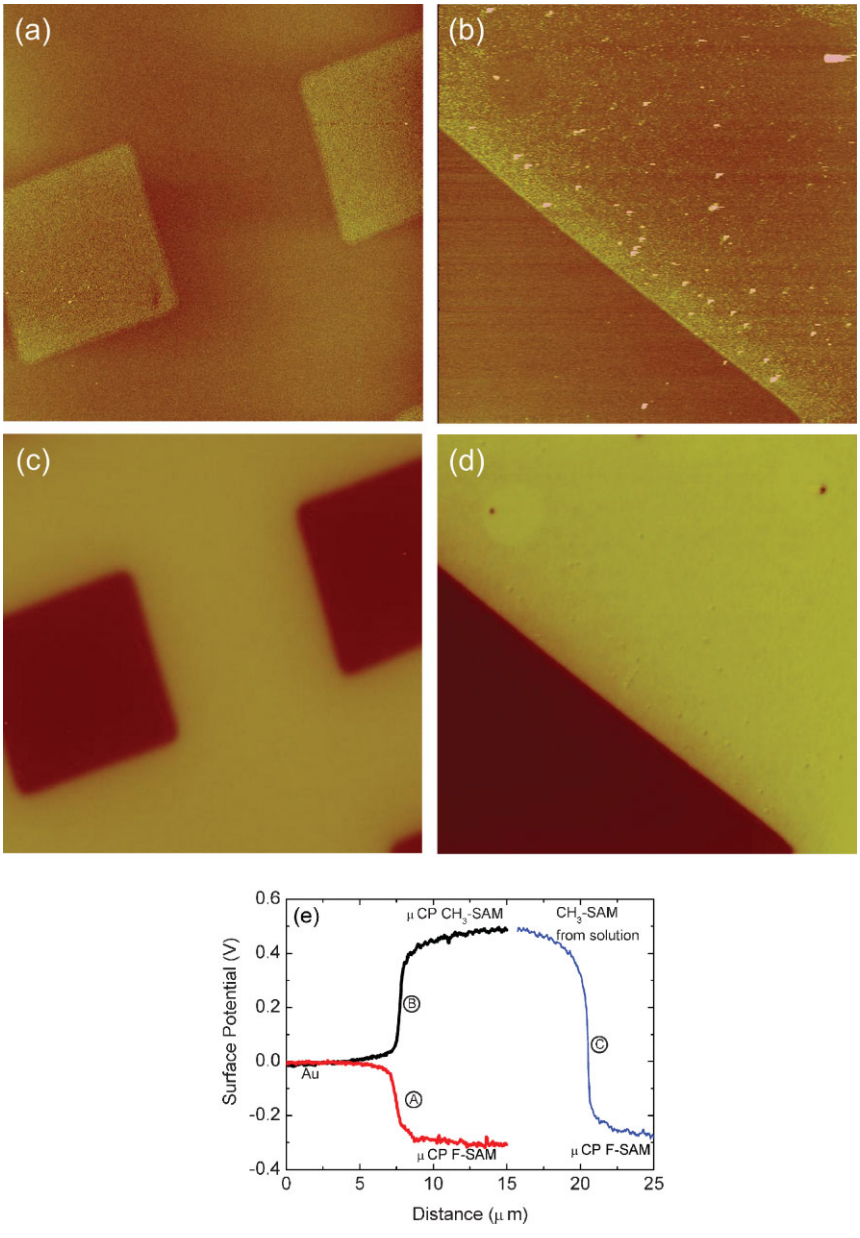

Figure 1. a,b) Topography of microcontact printed $C_4F_9C_{12}H_{24}SH$ and $C_{18}H_{37}SH$, respectively. The area of the pictures is 25×25 μm^2, the height scale is 15 nm. c,d) Surface potentials belonging to the topographies of (a) and (b), respectively. e) Cross-section of the surface potentials for the microcontact-printed F-SAM and CH_3-SAM on Au. The right curve is the surface potential of the printed F-SAM after immersing it in a solution of $C_{18}H_{37}SH$ in ethanol.

molecules of 0.5 V and −0.3 V for the CH_3-SAM and F-SAM are smaller than the calculated changes in surface potential and also smaller than surface potential changes obtained using monolayer formation from solution, which are 0.8 V and −0.6 V for the CH_3-SAM and F-SAM, respectively.[12] The printed monolayer is not anticipated to be perfectly dense or aligned, and therefore lower values for the surface potential change can be expected. In addition, the deviation of the measured from the calculated work function change might also be attributed to depolarization effects at the interface, which tend to reduce the dipole moment of the individual molecules.[17] Moreover, owing to the capacitive coupling between the AFM probe and the substrate, the measured surface potential difference should be regarded as a lower limit.[18]

To increase the local contrast in patterned OLEDs, we first printed the F-SAM. Then we immersed the substrate with the printed F-SAM in a 2 mM ethanol solution of $C_{18}H_{37}SH$ for 1 min. In this manner a contrast in work function as large as 0.8 eV (Fig. 1e, curve C) was obtained. This is in agreement with the sum of the work functions for the separate molecules printed on gold and indicates that the printed self-assembled monolayer does not dissolve into the solution. The work function contrast of 0.8 eV suggests that the intermixing of the two molecules is negligible, despite the imperfect packing of the F-SAM. Moreover, the edges are sharp and from the surface potentiometry we deduce a lateral transition region on the order of 100 nm or less. The concept of changing the work function of the electrode allows the change of the injection barrier of an OLED by changing the anode work function using a SAM. Additionally, by patterning the SAMs, we pave the way to the fabrication of patterned OLEDs with enhanced (or reduced) light emission on a nanometer scale. This straightforward fabrication method has the additional advantage that it does not require the use of expensive and time-consuming lithography.

In Figure 2a and b we present optical microscopy images of patterned OLEDs based on printed CH_3-SAMs and F-SAMs. Both consist of 100 nm Al/5 nm Ba/80 nm OC_1C_{10}-PPV/SAM/20 nm Au, in which OC_1C_{10}-PPV is poly[2-methoxy-5-(3′,7′-dimethyloctyloxy)-1,4-phenylene vinylene]. The thickness of the light-emitting polymer is not affected by the presence of the self-assembled monolayer. In Figure 2a, the squares were printed using a CH_3-SAM, and a negative image is obtained. In Figure 2b, the same squares were printed with a F-SAM, creating a positive image. The squares are $10 \times 10\,\mu m^2$. We observe that in the case of the CH_3-SAM the printed area is dark; in case of the F-SAM the printed area is bright. These observations are in agreement with the direction of the dipole moment and the change in work function corresponding to this dipole orientation. Note that the devices based on the F-SAMs can only produce a patterned light emission because of the presence of an injection barrier for holes at the pristine Au/OC_1C_{10}-PPV interface (see Fig. 3b).

To study the charge transport, we have prepared OLEDs with anodes of gold that were completely covered with a

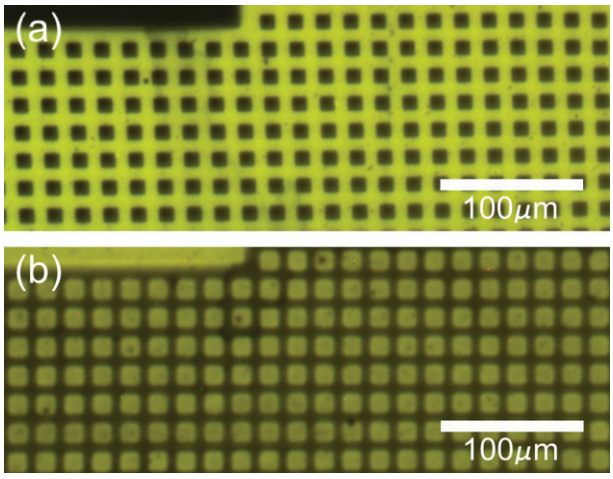

Figure 2. Optical microscopy image of a light-emitting diode with a patterned anode using a printed self-assembled monolayer consisting of a) a CH_3-SAM and b) a F-SAM. The squares on the pictures are $10 \times 10\,\mu m^2$.

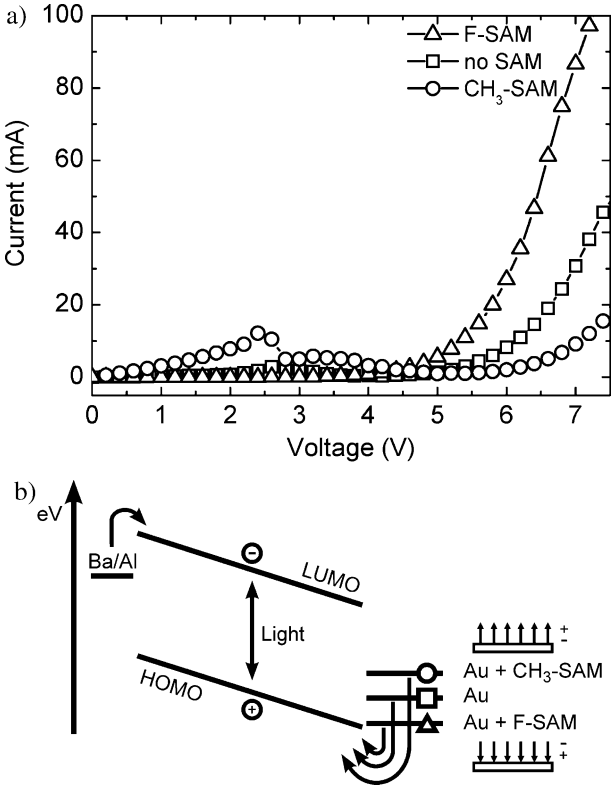

Figure 3. a) Current as a function of voltage for three OLEDs with a CH_3-SAM (squares), F-SAM (circles), and without a SAM (triangles) on the Au electrode. b) Band diagram of an OLED consisting of a Ba/Al cathode, an OC_1C_{10}-PPV organic layer, and a Au anode. The (local) work function of the anode can be altered with a self-assembled monolayer to in- or decrease the barrier for hole injection. The right-hand side of the picture shows a schematic representation of the orientations of the dipoles for the F-SAM and CH_3-SAM on Au.

ADVANCED MATERIALS

CH_3-SAM, a F-SAM, and OLEDs without SAM. The current as a function of voltage for the three devices is plotted in Figure 3a. We observe that the current in the F-SAM device exceeds the current of the device without a SAM. In the device with a CH_3-SAM the current is reduced. A band diagram of the OLED is presented in Figure 3b. The Ba/Al and the Au electrodes are shown on the left- and right-hand side, respectively. A layer of OC_1C_{10}-PPV is sandwiched in between. The F-SAM improves the injection of holes because the barrier between the gold contact and the OC_1C_{10}-PPV is reduced. The CH_3-SAM, on the other hand, increases the energy level of the Au electrode with respect to the polymer HOMO level and therefore hampers the hole injection. Thus, by changing the work function, we effectively change the injection barrier and therefore the current balance in the diode. By changing the energy levels, the built-in voltage, that is, the difference between the work function of the anode and cathode, is also changed. Figure 3a shows that decreasing the built-in voltage has a smaller effect on the current than changing the injection barrier. We note that an anomaly at low voltages is observed. This anomaly in the current has been observed more frequently in OLEDs.[19,20] Furthermore, it has recently been shown that the luminous efficiency can be improved by using a SAM that reduces the exciton quenching effect through nonradiative energy transfer to the metal electrode.[21–22] This effect occurs in addition to the work function change. We observe a decrease in the light emission in Figure 2a for the CH_3-SAM. The effect on the light emission of the change in work function caused by the SAM is therefore bigger than the effect of the reduced quenching.

In summary, we have shown the production of patterned organic light-emitting diodes by a simple microcontact printing technique. We have used two molecules of only 2 nm with opposing dipole directions, which orient themselves on gold and therefore change the local work function. We have quantified this difference in work function with scanning Kelvin probe microscopy and, by applying a monolayer of these molecules on the anode of a light-emitting diode, we can control the local hole injection, resulting in a direct handle on the local light emission. The work function can be modulated within a resolution smaller than 100 nm, allowing a straightforward and low-cost fabrication process for structuring OLEDs on nanometer length scales.

Received: January 30, 2008
Revised: March 3, 2008
Published online: June 2, 2008

[1] W. Osikowicz, M. P. de Jong, S. Braun, C. Tengstedt, M. Fahlman, W. R. Salaneck, *Appl. Phys. Lett.* **2006**, *88*, 193504.
[2] T.-W. Lee, J. Zaumseil, Z. Bao, J. W. P. Hsu, J. A. Rogers, *Proc. Natl. Acad. Sci. USA* **2004**, *101*, 429.
[3] T. van Woudenbergh, P. W. M. Blom, J. N. Huiberts, *Appl. Phys. Lett.* **2003**, *82*, 985.
[4] R. J. Jackman, J. L. Wilbur, G. M. Whitesides, *Science* **1995**, *269*, 664.
[5] J. D. Jackson, *Classical Electrodynamics*, Wiley, Chichester, UK **1999**, p. 41.
[6] D. M. Taylor, O. N. De Oliviera, Jr., H. J. Morgan, *J. Colloid Interface Sci.* **1990**, *139*, 508.
[7] R. J. Demchak, T. Fort, Jr., *J. Colloid Interface Sci.* **1974**, *46*, 191.
[8] P. C. Rusu, G. Brocks, *J. Phys. Chem. B* **2006**, *110*, 22628.
[9] P. C. Rusu, G. Brocks, *Phys. Rev. B* **2006**, *74*, 073414.
[10] V. De Renzi, R. Rousseau, D. Marchetto, R. Biagi, S. Scandolo, U. del Pennino, *Phys. Rev. Lett.* **2005**, *95*, 046804.
[11] R. W. Zehner, B. F. Parsons, R. H. Hsung, L. R. Sita, *Langmuir* **1999**, *15*, 1121.
[12] B. de Boer, A. Hadipour, M. M. Mandoc, T. van Woudenbergh, P. W. M. Blom, *Adv. Mater.* **2005**, *17*, 625.
[13] L. Bürgi, H. Sirringhaus, R. H. Friend, *Appl. Phys. Lett.* **2002**, *80*, 2913.
[14] V. Palermo, M. Palma, P. Samori, *Adv. Mater.* **2006**, *18*, 145.
[15] M. Nonnenmacher, M. P. O'Boyle, H. K. Wickramasinghe, *Appl. Phys. Lett.* **1991**, *58*, 2921.
[16] D. M. Alloway, M. Hofmann, D. L. Smith, N. E. Gruhn, A. L. Graham, R. Colorado, Jr., V. H. Wysocki, T. Randall Lee, P. A. Lee, N. R. Armstrong, *J. Phys. Chem. B* **2003**, *107*, 11690.
[17] D. Cornil, Y. Olivier, V. Geskin, J. Cornil, *Adv. Funct. Mater.* **2007**, *17*, 1143.
[18] G. Koley, G. Spencer, H. R. Bhangale, *Appl. Phys. Lett.* **2001**, *79*, 545.
[19] S. Berleb, W. Brütting, M. Schwoerer, *Synth. Met.* **1999**, *102*, 1034.
[20] F. Verbakel, S. C. J. Meskers, R. A. J. Janssen, H. L. Gomes, M. Cölle, M. Büchel, D. M. de Leeuw, *Appl. Phys. Lett.* **2007**, *91*, 192103.
[21] T.-W. Lee, *Adv. Funct. Mater.* **2007**, *17*, 3128.
[22] T.-W. Lee, J. W. P. Msu, *Appl. Phys. Lett.* **2006**, *89*, 223511.